ELSEVIER

An Experimental Study of Condensation Heat Transfer in a Horizontally Rotating Cylinder with a Scraper

S. W. Peng

K. Mizukami
Department of Mechanical Engineering, Ehime University, Matsuyama 790, Japan

W. Liu
Huazhong University of Science and Technology, Wuhan, People's Republic of China

N. Sebe
Mitsubishi Electric Company, Kobe

T. Takeba
Toshiba Company, Tokyo

■ Film condensation on the inside wall of a horizontally rotating cylinder with a scraper is studied experimentally for both thin and thick films. For either case, four distinct hydrodynamic regimes are observed: an unsteady gravitational flow regime at low rotational Reynolds number with accumulation; a nonboundary layer regime with bore as rotational Reynolds number is increased; a filmlike regime with ripples as rotational Reynolds number is further increased; a rimming film regime without obvious waves as the rotational Reynolds number exceeds a certain value. It is noted that the heat transfer coefficient increases with increasing rotational Reynolds number in all three quasi-steady regimes for the thin film case. For the thick film case, the heat transfer coefficient increases in both the bore and the ripples regimes but decreases in the rimming regime with increasing rotational Reynolds number, with a maximum heat transfer coefficient obtained in the ripples regime. The transport mechanism is analyzed, and a comparison is made between the experimental results and the theory of solid film. © *Elsevier Science Inc., 1997*

Keywords: *rotating cylinder, scaper, film condensation, heat transfer, hydrodynamics*

INTRODUCTION

The rotational cylinder condenser is widely used in paper mills as a paper drum. Steam is fed into a rotating cylinder, on the outer surface of which moist paper is bound and is caused to move with the cylinder surface. Because the temperature of the moist paper is lower than the saturation temperature of steam, the vapor condenses. As a result, a condensate film is formed.

The condensate is usually removed by siphons [1], but here the condensate film is usually quite thick, which increases both the thermal resistance and the mechanical load for rotation. To overcome this difficulty, Futagami et al. [2] first proposed to use a scraper to remove the condensate mechanically. Since then, a lot of theoretical and experimental work has been performed to analyze the heat transfer characteristics in film condensation on the inside surface of a rotating cylinder.

The theoretical models developed may be broadly classified in two categories: the gravity model and the centrifugal force model. In the gravity model, the condensate flow is taken to be dominated by gravity. The model neglects the pressure gradient. The balance of gravity and viscosity, together with energy conservation, determines the distributions of velocity and film thickness, as well as the heat transfer coefficient. The so-called laminar model by Futagami et al. [2], the improved laminar model by Mizukami et al. [3], and the turbulent model by Peng and Mizukami [4] fall into this class. In the centrifugal force model, the condensate flow is taken to be dominated by centrifugal force. In contrast with the gravity model, the centrifugal force model neglects the effect of gravity and considers that the centrifugal force produces a pressure gradient in the condensate film, which causes the condensate to flow. Recent work by Peng and Mizukami [5] falls into this class.

The experimental results reported in Mizukami et al. [3] and Peng and Mizukami [4] show the effect of the residual film thickness on the heat transfer coefficient. However, to the present, no detailed experimental results have been reported on the effect of rotational Reynolds number on the heat transfer coefficient and on the evolution of wave shape and position.

The purpose of this paper is to present the experimental results of film condensation on the inside wall of a rotating paper drum with a scraper for both thin and thick films with particular attention paid to the effect of the

Address correspondence to Dr. Shi-Wen Peng, Laboratoire de Thermocinetique, ISITEM, La Chantrerie, C.P. 3023, 44087 Nantes Cedex 03, France.

Experimental Thermal and Fluid Science 1997; 14:205–212
© Elsevier Science Inc., 1997
655 Avenue of the Americas, New York, NY 10010

0894-1777/97/$17.00
PII S0894-1777(96)00076-3

rotational Reynolds number on the heat transfer and hydrodynamic characteristics of the condensate film.

APPARATUS AND MEASUREMENT

Apparatus

The experimental apparatus is nearly the same as the one described in Futagami et al. [2], but here we allow a residual film thickness to exist at the scraper position, as shown in Fig. 1.

The vapor of R113 generated in an evaporator is led into a rotating stainless steel cylinder that is 312 mm in inner diameter, 378 mm in length, and 3.83 mm in wall thickness. The cylinder is horizontally positioned and supported from both ends by roller bearings. The whole cylinder is divided into three sections, the middle one of which is the test section, with a subsection at each end. The end plates are made of transparent acrylic resin, allowing observation of the flow states of the condensate in the cylinder. One end plate is coupled to a variable-speed motor. The subsections are separated from the test section by two 40 mm high by 3 mm wide strips that are positioned 65 mm from either end, the purpose of which is to diminish the end effect. Therefore, the test section is 248 mm in length. The pressure in the cylinder is maintained slightly higher than atmospheric pressure. The cylinder is cooled by environmental air.

The scaper itself is made of rubber. It is separated from the inner surface of the cylinder by two ball pen tips. The ball pen tips are buried in bolts that are screwed to the scaper. The clearance between the scaper and the inner surface can be regulated by adjusting the bolts.

The condensate is scraped at the top of cylinder. The scraped condensate flows down through two tubes, which also serve as support for the whole scraper, to the shaft. The shaft, about which the cylinder rotates, is fixed. The condensate finally flows through the shaft, by a flowmeter, to the reservoir. The condensate in the subsections is conducted directly into the reservoir. The small amount of vapor that may be carried by the condensate is caused to flow into the subreservoir first, where the vapor condenses, and then into the absorber, which contains water. The vapor is conducted into and absorbed by the water. The remnant vapor is released into the atmosphere. The condensate in the reservoir is pumped into the evaporator (to be evaporated again). The condensate in the subreservoir is removed manually and placed in the evaporator from time to time.

Measurement

Before the experiment, an initial residual film thickness must be set up. As stated above, the residual film thickness can be regulated by adjusting the bolts where the ball pen tips are affixed. After an initial residual film thickness has been set up, its exact value is measured by chink gauges. Every residual film thickness is measured at 40 positions (five different circumferences along the axis and eight different positions along every circumference). An average of all these measurements is taken as the final value of residual film thickness. Other measurements are made only after the condensation and scraping becomes quasi-steady, which is marked by a steady temperature difference between vapor and wall.

The flow rate is obtained by measuring the time that it takes the scraped condensate to fill up a certain volume in the flowmeter. The pressure is measured by a manometer.

Tempeatures are measured by thermocouples. A K-type thermocouple [6] is affixed to a thin rod that extends into the vapor space in the cylinder. The temperature obtained is regarded as the vapor saturation temperature. Because the temperature difference between the vapor and the cylinder wall is small (about 0.058–0.79C°), the temperature difference is measured directly by an E-type thermocouple [6] of 0.1 mm in diameter. Thermocouples are

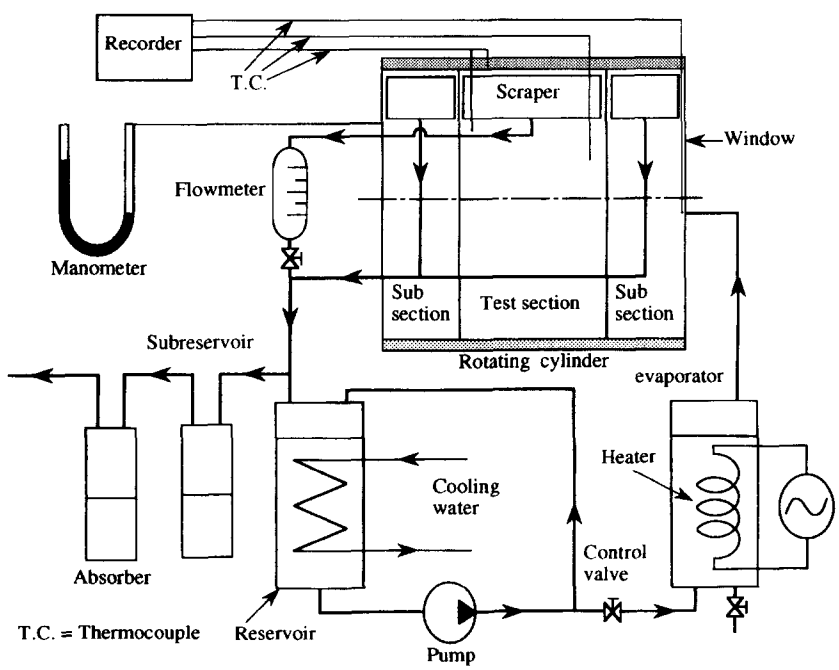

Figure 1. Diagram of experimental apparatus.

mounted at five different positions in the cylinder wall, with one end at a depth of 2 mm from the outer surface and the other end exposed to the vapor space in the cylinder at a distance of 40 mm from the inner surface. To increase the thermoelectric potential of the thermocouple, the five thermocouples are linked in series to form a thermopile. The two ends of the thermopile are mounted on slip rings with mercury contact. The temperature difference can be obtained by measuring the difference between the thermoelectric potentials at the mercury contacts.

The number of revolutions is measured by a CdS photoelectric detector. A small piece of matted tape is mounted on the outer surface of the cylinder. A pulse signal is obtained by using a photoelectric detector, from which the number of revolutions can be obtained.

Waves on the condensate film can be observed through the transparent end plate of the cylinder. When the flow becomes steady waves are observed at relatively fixed positions. A scaled disk is used to read the positions of the waves. The wave shape and position are observed by the naked eye. Several photographs of waves are taken during the experiments.

DATA REDUCTION

The condensation rate is obtained by measuring the time, τ, for the condensate to fill up a given volume, V, of the flowmeter:

$$m = \rho_f \frac{V}{\tau}, \tag{1}$$

where ρ_f is the density of the condensate.

The heat flux is obtained from the condensation rate:

$$q = \frac{m h_{fg}}{2\pi R L}, \tag{2}$$

where R is the inner radius of the cylinder, L is the length of test section, and h_{fg} is the latent heat of condensation.

The temperature difference across the condensate film is obtained by the energy balance along the radial direction under the assumption of one-dimensional heat transfer in the radial direction:

$$t_s - t_w = (t_s - t_{wm}) - \frac{qd}{\lambda_w}, \tag{3}$$

where d is the distance between the low-temperature junction buried in the wall and the inner surface λ_w is the thermal conductivity of the cylinder wall (SUS304 stainless steel), t_s is the vapor saturation temperature t_{wm} is the temperature in the middle of wall where the low-temperature junctions of thermocouples are buried and t_w is the temperature of the inner surface.

The average heat transfer coefficient, k, and its dimensionless form, K, are defined as

$$k = \frac{q}{t_s - t_w}, \qquad K = \frac{kR}{\lambda_f}, \tag{4}$$

respectively. Here λ_f is the thermal conductivity of the condensate. All the thermal properties are taken to be constant. For R113, the values at saturation temperature are taken, but, for the cylinder, the values at the inside wall temperature are used.

Uncertainties were estimated by the method suggested by Moffat [7]. They are $\pm 15.2\%$ for the heat transfer coefficient. The main causes of the uncertainties in the heat transfer coefficient are the uncertainties in the temperature difference between the vapor and the inner surface. The uncertainties in the condensate rate, the area of test section, and the rotational Reynolds number were found to be negligible.

The uncertainties from the one-dimensional heat transfer assumption in data reduction, the noncondensable gases, and the system vibration during rotation are neglected in the uncertainty analysis. The effect of the one-dimensional heat transfer assumption is expected to be very small for a film condensation problem [8]. The effect of the noncondensable gases is reduced by feeding vapor into the cylinder and maintaining a slightly positive pressure for a period of time before measurement to expel the air in the cylinder. This source of error tends to reduce the heat transfer coefficient. The system vibration may affect the heat transfer coefficient through affecting the distributions of the velocity and film thickness of the condensate. It is expected that the system vibration may slightly raise the heat transfer coefficient.

Because the temperature of vapor is higher than that of the environment, it is expected that there is axial heat conduction along the shaft of cylinder. Therefore, the temperatures of the two slip rings may be different, even at the same radial distance where the two ends of thermopile are fixed. To compensate for the error incurred by the axial heat conduction, experiments were performed to obtain the error incurred by the cross wiring of the two slip rings and the two ends of the thermopile. The error is found to be a function of the temperature difference between vapor and environment:

$$\varepsilon = 0.95 \times 10^{-7}(t_{ts} - t_a)^{3.9}. \tag{5}$$

Here t_a is the temperature of the environment. The maximum error due to this source is 0.2C°.

Therefore, for the wiring in the experiments, the temperature difference across the condensate film can finally be obtained by modifying Eq. (3) to include the preceding error:

$$t_s - t_w = (t_s - t_{wm}) - \frac{qd}{\lambda} + \frac{\varepsilon}{2}. \tag{6}$$

EXPERIMENTAL RESULTS AND DISCUSSION

Four different flow modes were observed. When the rotational speed is very low, the condensate flows down on the inner surface of the horizontally rotating cylinder from both the upward and the downward sides (the flow rate of the upward side is less than that of the downward side), under the influence of gravity, to form an accumulation at the bottom of the rotating cylinder. When the rotational speed is increased, the accumulation is replaced by a bore at the upward side of horizontally rotating cylinder, with a thickness comparable to the film thickness. The bore moves upward as the rotational speed is continuously increased, with the thickness of the bore decreasing. As the rotational speed is further increased, the bore disappears. Instead, some small waves, so-called ripples, appear

on the upward top portion of the cylinder. In contrast with the bore thickness, the amplitude of the ripples is small compared with the film thickness. When the rotational speed exceeds a certain limiting value, the ripples disappear, and a rimming film forms. The positions at which the bore and ripples appear are shown in Fig. 2 for dimensionless residual film thickness $\Lambda = 1.9 \times 10^{-3}$.

Heat transfer measurements are made only for the three steady-flow modes—that is, bore, ripples, and rimming regimes.

The variations of the heat transfer coefficient with respect to the rotational Reynolds number are shown in Fig. 3 for one thin-residual-film case with the dimensionless residual thickness Λ equal to 1.2×10^{-3}, and in Fig. 4for three thick-film cases with Λ equal to 1.7×10^{-3}, 1.9×10^{-3} and 2.4×10^{-3}, respectively.

Note that the variations of heat transfer coefficient with respect to the rotational Reynolds number differ according to the residual film thickness. As shown in Figs. 3 and 4, for the thin-film case, the heat transfer coefficient increases with increasing rotational Reynolds number in all three steady regimes; but, for the thick-film cases, the heat transfer coefficient increases in both the bore and the ripples regimes but decreases in the rimming regime with increasing rotational Reynolds number. The decrease in residual film thickness results in a significant increase in the heat transfer coefficient, because the heat transfer resistance is greatly reduced.

In contrast with condensation on the outer surface of a rotating cylinder [9, 10], the Weber number not important in our problem, because the condensate cannot be thrown off and surface tension plays no role (provided the surface tension–induced flow of condensate is negligible). Therefore, the Froude number is the only important parameter for judging whether the flow is gravity dominated or centrifugal force dominated. For $0 < \mathrm{Fr} < 1$, the flow is dominated by gravity, and the gravity model is applicable. For $\mathrm{Fr} \gg 1$, the effect of gravity can be neglected, and the flow is dominated by centrifugal force, making the centrifugal force model applicable. In the intermediate

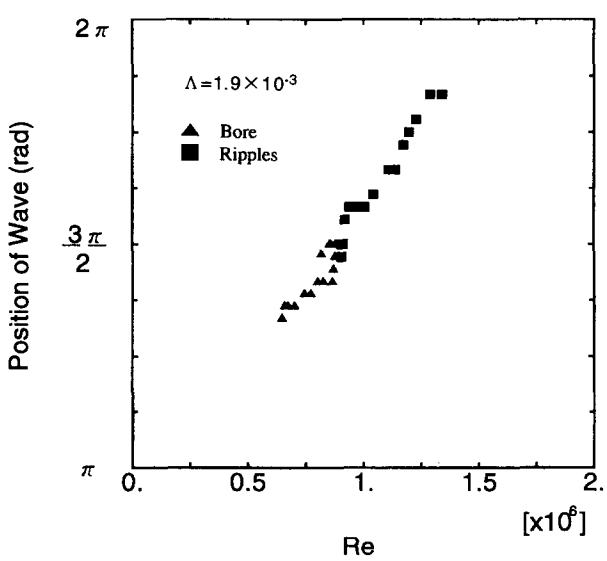

Figure 2. Positions of waves for $\Lambda = 1.9 \times 10^{-3}$.

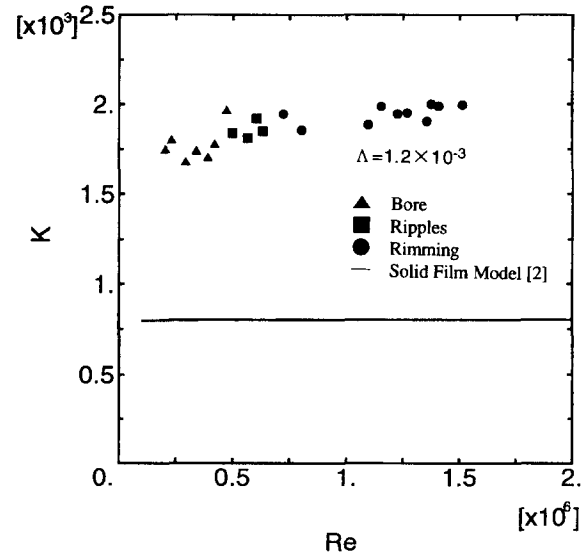

Figure 3. Effect of Re on the heat transfer coefficient for the thin-film case ($\Lambda = 1.2 \times 10^{-3}$).

regime, the gravity and centrifugal force are of equal importance, both of which should be included in the analysis.

The gravity model may be applied even in the bore regime for thin-film cases in which the condition $\mathrm{Fr} < 1$ is satisfied. However, the effect of centrifugal force has to be considered for ripples and rimming regimes. For thick-film cases, the transition from accumulation mode to bore mode takes place at a higher rotational Reynolds number, which makes the condition $\mathrm{Fr} < 1 <$ untenable.

The heat transfer coefficient generally depends on the rotational Reynolds number, Re, the Prandtl number, Pr, the Froude number, Fr [11], the Stefan number, Ste, and the dimensionless residual thickness, Λ [5]. The film thickness generally decreases with an increase in rotational Reynolds number. When the film is very thin, turbulence does not develop due to the constraint effects of wall and surface tension, and so the heat transfer coefficient increases monotomically with the increase in the rotational Reynolds number. When the film is thick, the development of turbulence becomes possible. When the rotational Reynolds number is increased, though the film thickness decreased the condensate is forced to rotate more and more like a rigid body, and so the viscosity influence regime is greatly thinned [12], and the turbulence may be damped down by the centrifugal force, which in turn reduces the heat transfer coefficient. Therefore a maximum heat transfer coefficient was obtained for a thick film.

Futagami et al.'s solid-film model [2] expresses the dimensionless heat transfer coefficient, K, as

$$K = \frac{\mathrm{Pr\,Re}\,\Lambda}{2\pi\,\mathrm{Ste}}\left(\sqrt{1 + \frac{4\pi\,\mathrm{Ste}}{\mathrm{Pr\,Re}\,\Lambda^2}} - 1\right). \tag{7}$$

The solid lines in Figs. 3 and 4 indicate the analytical results from the solid-film model. As shown in the figures, the predicted values are about one-half of those obtained by experiments. In experiments, the temperature differ-

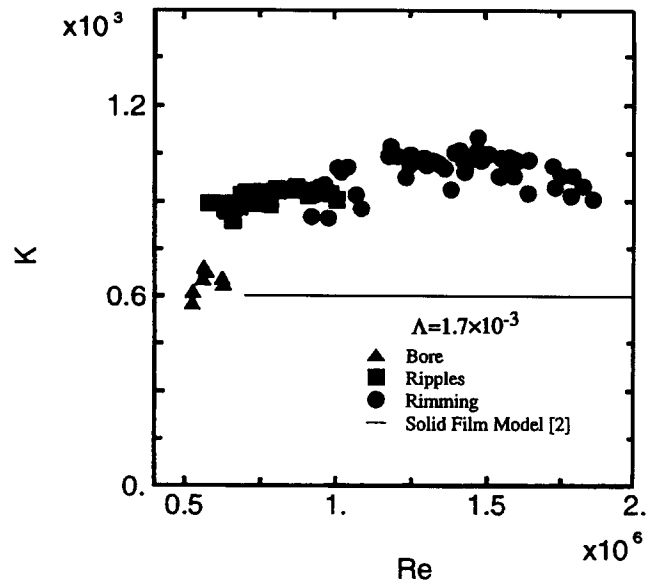

(a)

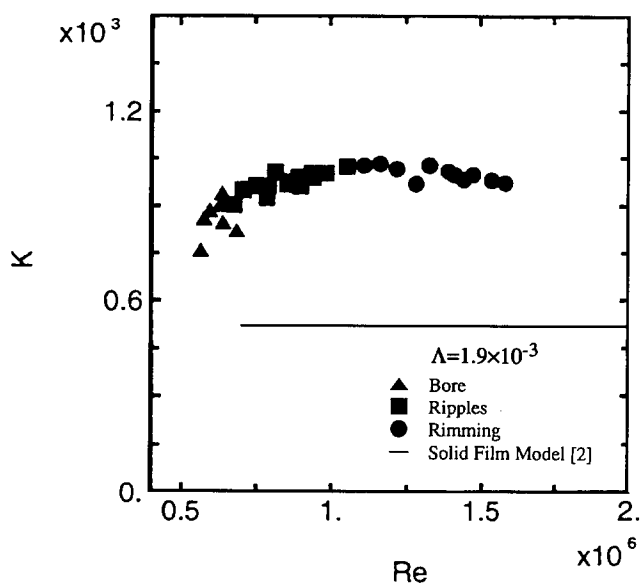

(b)

Figure 4. Effect of Re on the heat transfer coefficient for the thick-film case: $\Lambda = 1.7 \times 10^{-3}$; $\Lambda = 1.9 \times 10^{-3}$; and $\Lambda = 2.4 \times 10^{-3}$.

ence across the film changes from 0.45 K to 0.65 K, with a total average value of 0.5 K. The corresponding Stefan number is 3.402×10^{-3}.

The typical aspects of bore and ripples are shown in Figs. 5 and 6, respectively. The 8.5cm × 12cm photographs were taken by a camera located outside the cylinder and next to the transparent end plate, which is in clockwise rotation if seen from the camera's position. A bore is something like a rolling wave in a falling film flow [13], but its position is fixed and the wall is moving. Ripples are small amplitude waves in the condensate film. An illustration of four flow regimes is given in Fig. 7.

The transition characteristics of flow regimes are observed in the experiment (Fig. 8). The thicker the residual

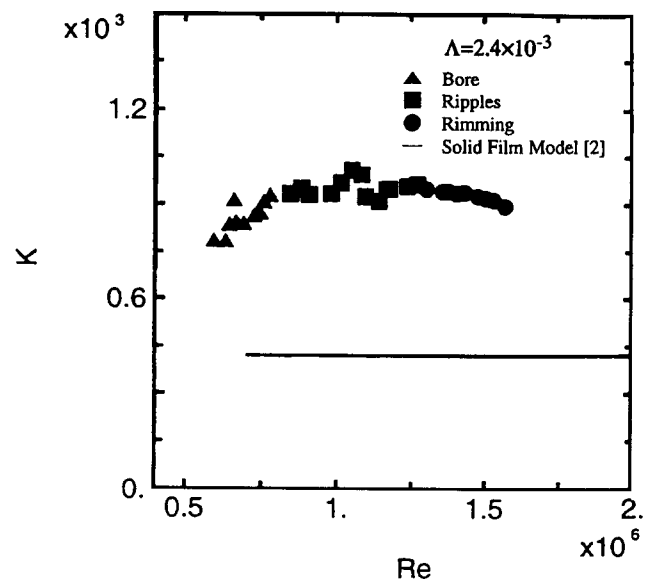

Figure 4. (*Continued*)

film, the larger the rotational Reynolds and Froude numbers at which the transitions from accumulation to bore, from bore to ripples, and from ripples to rimming take place. The transitions were observed for two cases by increasing and decreasing the rotational speed. Hysteresis was found for the transitions between bore and ripples and between ripples and rimming, and the critical rotational Reynolds numbers for the transitions from a higher speed mode to a lower speed mode are less than those for the transitions from a lower speed mode to a higher speed mode. When a ripples or rimming regime has been established, the cylinder speed may be decreased considerably below the critical speed at which the transition from bore to ripples or from ripples to rimming occurs.

PRACTICAL SIGNIFICANCE

In a paper mill, most of the steam is consumed in the drying process. Therefore, any improvement in the paper drying drum will result in an appreciable energy saving.

Figure 5. Photograph of a bore.

Figure 6. Photograph of ripples.

The present work advanced the investigation undertaken by Futagami et al. [2] to develop a paper drying drum of high efficiency.

That a paper drying drum with a scraper and those with siphons have the same hydrodynamic characteristics but different heat transfer characteristics may be of interest to engineers in industry. The flow regimes observed in the present experiments are nearly the same as those reported by White [14], White and Higgins [15], and Appel and Hong [16] for a paper drying drum with siphons. However, the heat transfer coefficient changes with the rotational Reynolds number in a different fashion. According to Appel and Hong [15], for the siphon case, the heat transfer coefficient decreases with an increase in the rotational Reynolds number in every flow regime, with a maximum heat transfer coefficient obtained at the low-speed flow mode, which differs from our observation that a maximum heat transfer coefficient exists in the ripples or rimming regime, even for the thick-film case. We consider that this is because the scraper can effectively reduce the condensate film thickness (when the rotational speed is raised) and therefore improve heat transfer across the condensate film, which offsets the unfavorable effect of turbulence or convection damping due to high-speed rotation, causing the maximum heat transfer coefficient to be obtained at a relatively high speed flow mode.

With a paper drum with siphons, it is usually very difficult to maintain a very thin condensate film, and a thin film is desirable for a good paper drier, especially at high-speed rotation. Rotational speed is an important parameter in a paper mill, because it determines the moving speed of paper and, therefore, the output per machine. A paper drying drum with good heat transfer performance in high-speed flow regimes may be very attractive to the paper industry.

CONCLUSIONS

Four distinct hydrodynamic and thermal regimes were observed:

1. At low rotational speeds ($0 \leq Fr < 1$), the condensate is drained by gravity and forms an accumulation at the bottom of the paper drum, with the heat transfer being unsteady.

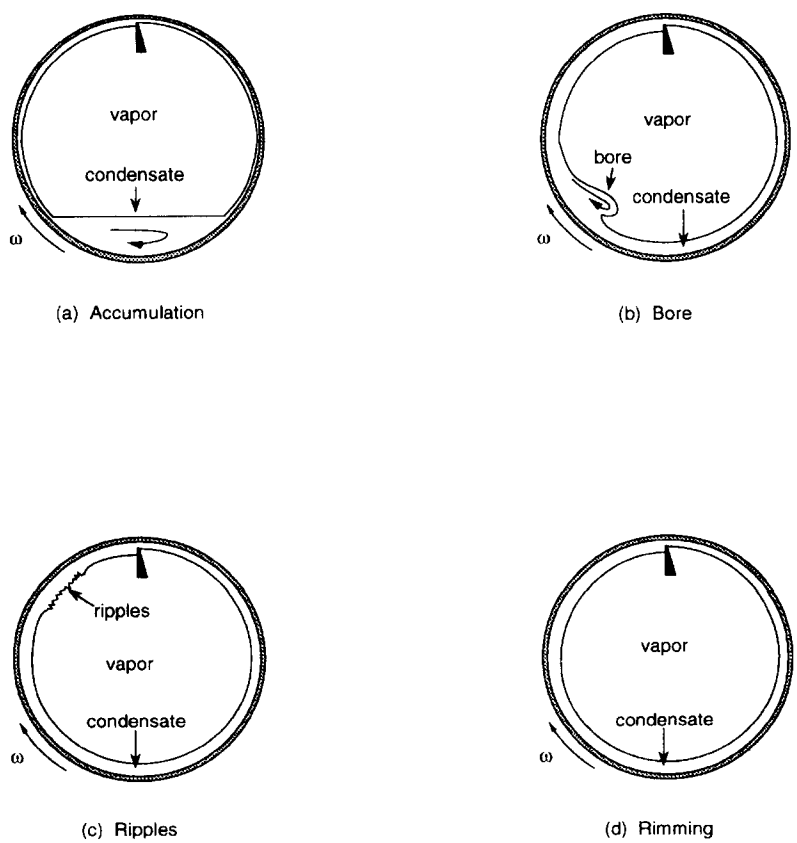

Figure 7. Diagrams of flow regimes.

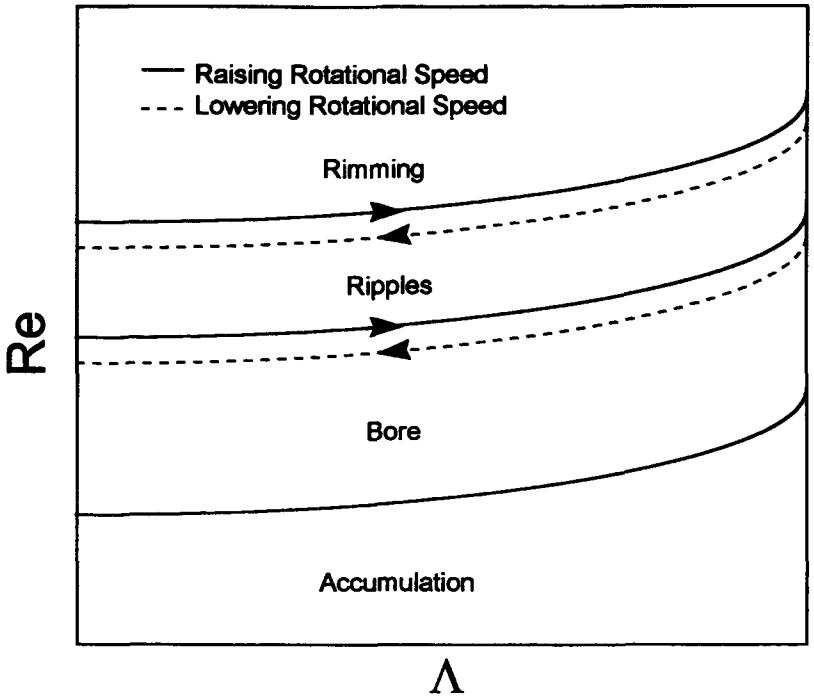

Figure 8. Transitions of flow regimes.

2. At moderate rotational speeds, a nonboundary layer bore forms on the upward side.
3. With the rotational speeds further increased, the bore is replaced by ripples.
4. At high rotational speeds, a rimming flow film forms.

The heat transfer coefficient increases monotonically as the rotational speed is increased for the thin-film case; but the heat transfer coefficient first increases and then decreases as the rotational speed is increased for the thick-film case, with a maximum heat transfer coefficient obtained at a certain intermediate rotational speed.

The thicker the residual film, the larger the Reynolds and Froude numbers at which the transition from a lower rotational speed mode to a higher speed mode happens.

A decrease in the residual film thickness results in a significant increase of the heat transfer coefficient. The heat transfer coefficient is about twice that estimated by the solid-film model.

Detailed measurements of the velocity and turbulence strength distributions and their variation with rotational speed will be very important for understanding the transport process in the rotational condensate film. New theoretical models for analyzing the effect of the waves and their interaction with the centrifugal force are also required. Considerable research has been undertaken in the past decades on the wave dynamics of a falling film, but little research has been reported in the literature dealing with the wave movement in a rotational film. Experimental research is also needed to examine the effects of fluid properties, surface characteristics of the cylinder, and the diameter of cylinder on the hydrodynamic and heat transfer characteristics of the mechanically scraping paper drying them.

Recent work by Mizukami et al. (17) shows possible unsteadiness in the lower-speed states, such as bore and ripple, though no unsteadiness was observed in the present experiment. Mizukami et al. reached their conclusion by comparing the outer convection heat transfer coefficient with previous experimental results in studies of the convection heat transfer coefficient of the rotating cylinder. Further experiments should be performed to confirm this observation. If the heat transfer is unsteady in a lower-speed state, it is expected that the wave positions (bore and perhaps ripple) may change with time—not appearing at the fixed position observed in this experiment (and reported by Futagami et al. [2] and Mizukami et al. [3]—if sufficiently long time observations are made.

NOMENCLATURE

C_p	specific heat of condensate, J/(kg K)
d	radial distance between the inner surface and the low-temperature junction, m
Fr	Froude number, $= \omega^2 R/g$, dimensionless
g	gravitational acceleration, m/s^2
h_{fg}	latent heat of evaporation, J/kg
k	heat transfer coefficient, W/(m^2 K)
K	heat transfer coefficient, kR/λ_f, dimensionless
L	length of test section, m
m	condensation rate, kg/s
Pr	Prandtl number of the condensate, ν/α, dimensionless
q	heat flux, W/m^2
Re	rotational Reynolds number, $\omega R^2/\nu$, dimensionless
R	inner radius of paper drum, m
Ste	Stefan number, $C_p(t_s - t_w)/h_{fg}$, dimensionless
t	temperature, K
V	volume of condensate, m^3

Greek Symbols

α thermal diffusivity of condensate, m^2/s
δ_b residual film thickness, m
ε error due to axial heat conduction, K
λ thermal conductivity, W/(m K)
Λ residual film thickness, δ_b/R, dimensionless
ν kinematic viscosity of condensate, m^2/s
ρ density, kg/m^3
τ time, s
ω rotational angular velocity, rad/s

Subscripts

a environment
f fluid
s saturation
w wall
wm low-temperature junction in the wall

REFERENCES

1. Roetzel, W., Improving Heat Transfer in Steam-Heated Fast Rotating Paper Drying Drums. *Int J. Heat Mass Transfer* **18**, 79–86, 1975.
2. Futagami, K., Ikeda, J., Ohhira, K., Aoyama, Y., and Mizukami, K., Condensation Heat Transfer in a Rotating Horizontal Cylinder with a Scraper. *Exp. Thermal Fluid Sci.* **2**, 384–391, 1989.
3. Mizukami, Yamazaki, Y., Aoyama, Y., and Futagami, K., A Laminar Analysis of Condensation in a Paper Drum with a Scraper. Proc. 1st Int. Conf. on Transport Phenomena in Processing, Honolulu, Hawaii, pp. 1537–1548, March 22–26, 1992.
4. Peng, S. W., and Mizukami, K., Turbulent Film Condensation on the Inside Wall of a Rotating Cylinder. Proc. Fourth ASME/JSME Thermal Eng. Joint Conf., Maui, Hawaii, pp. 375–382, March 19–24, 1995.
5. Peng, S. W., and Mizukami, K., Condensate Flow Induced by Centrifugal Force. In *Heat Transfer in Thin Films*, S. T. Thynell and A. F. Emery, Eds., ASME HTD Vol. 293, pp. 33–37, ASME, 1994.
6. *JSME Data Book*: *Heat Transfer*. 4th ed., JSME, Tokyo, 1986, in Japanese.
7. Moffat, R. J., Describing the Uncertainties in Experimental Results. *Exp. Thermal Fluid Sci.* **1**, 3–17, 1988.
8. Al-Baroudi, H. M., and Klein, A. C., Experimental Simulations and Heat Transfer Parameter Measurements of Film Condensation on a Rotating Flat Plate. *Exp. Thermal Fluid Sci.* **10**, 124–235, 1995.
9. Singer, R. M., and Prekshot, G. W., The Condensation of Vapor on a Horizontal Rotating Cylinder. *Proc. Heat Transfer Fluid Mech. Inst.* **14**, 205–221, 1963.
10. Nicol, A. A., and Gasesa, M., Condensation of Steam on a Rotating Vertical Cylinder. *Trans. ASME J. Heat Transfer* **92**, 144–151, 1970.
11. Ozerdem, B., and Toksoy, M., An Experimental Study of Convective Heat Transfer in a Partially Filled and Horizontally Rotating Cylinder. *Int. Comm. Heat Mass Transfer* **20**, 579–583, 1993.
12. Phillips, O. M., Centrifugal Waves. *J. Fluid Mech.* **7**, 340–352, 1960.
13. Lin, S. P., and Wang, C. Y., Modeling Wavy Film Flows. In *Encyclopedia of Fluid Mechanics*, N. P. Cheremisinoff, Ed., Vol. 1, pp. 931–951, Gulf Publishing, Houston, 1986.
14. White, R. E., Residual Condensate, Condensate Behavior, and Siphoning in Paper Driers. *TAPPI* **39**, 228–233, 1956.
15. White, R. E., and Higgins, T. W., Effect of Fluid Properties on Condensate Behavior. *TAPPI* **41**(2), 71–76, 1958.
16. Appel, D. W., and Hong, S. H., Condensate Distribution and its Effects on Heat Transfer in Steam-Heated Dryers. *Pulp Paper Magazine Can.* **T51**, 66–77, 1969.
17. Mizukami, K., Sebe, N., Abe, F., Peng, S. W., and Zhong, M. K., Flow Regimens in Film Condensation in a Horizontal, Slowly Rotating Cylinder. In *Rotating Machinery 1996*, D. C. Han, and J. H. Kim, Eds., Vol. 2 (*Transport Phenomena*) pp. 414–427, Sixth Proc. Int. Symp. on Transport Phenomena and Dynamics of Rotating Machinery, ISROMAC-6, Honolulu, Hawaii, 1996.

Received March 20, 1995; revised May 9, 1996